

Novel GSK-3 β inhibitors from sequential virtual screening

Hye-Jung Kim,^{a,b} Hyunah Choo,^a Yong Seo Cho,^a Kyoung Tai No^b and Ae Nim Pae^{a,*}

^aLife Science Division, Korea Institute of Science and Technology, PO Box 131, Cheongryang, Seoul 130-650, South Korea

^bDepartment of Biotechnology, Yonsei University 220, Sinchon-dong, Seodaemun-gu, Seoul 120-749, South Korea

Received 28 August 2007; revised 15 October 2007; accepted 16 October 2007

Available online 22 October 2007

Abstract—Glycogen synthase kinase-3 (GSK-3 β) has been emerging as a key therapeutic target for type-2 diabetics, Alzheimer's disease, cancer, and chronic inflammation. For the purpose of finding biologically active and novel compounds and providing new idea for drug-design, we performed virtual screening using commercially available database. Three-dimensional common feature pharmacophore model was developed by using HipHop program provided in Catalyst software and it was used as a query for screening database. Recursive partitioning (RP) model was developed as a filtering system, which was able to classify active and inactive compounds. Eventually, a sequential virtual screening procedure (SQSP) was conducted by applying the common feature pharmacophore and RP model in succession to discover novel potent GSK-3 β inhibitors. The final 56 hit compounds were carefully selected considering predicted docking mode in crystal structures. Subsequent enzyme assay for human GSK-3 β protein confirmed that three compounds of these hit compounds exhibit micromolar inhibitory activity. Here, we report novel hit compounds and their binding mode in the active site of GSK-3 β crystal structure.

© 2007 Elsevier Ltd. All rights reserved.

1. Introduction

Glycogen synthase kinase-3 is a regulatory serine/threonine kinase playing key roles in transduction of regulatory and proliferative signals arising at the cell membrane.¹ There are two highly homologous isoforms, named GSK-3 α and GSK-3 β , sharing 98% homology in their catalytic domain.² Both are constitutively active in resting cells, but their differential expression and the lack of relation between transcription and translation in some tissues indicate that GSK-3 α and GSK-3 β have different means of regulation.³ GSK-3 was originally identified as a regulator of glycogen synthase (GS) catalyzing the synthesis of glycogen.⁴ The facts that elevated GSK-3 activity was found in diabetic tissues support GSK-3 as a promising therapeutic target for insulin resistance and type-2 diabetes.^{5,6} Recent studies suggested that GSK-3 β is the *in vivo* player contributing to hyperphosphorylation of tau protein and it mediates increased production and aggregation of amyloid- β peptides. These observations imply a central role for GSK-3 β in Alzheimer's disease.^{7,8} There are experimental

evidences that GSK-3 β inhibitors lead to decreased cancer cell proliferation and survival via negative regulation of NF- κ B activity, p53-dependent apoptosis, and enhancing the TRAIL-induced cell death.^{9–11} In addition, the phosphorylation of proteins by GSK-3 β is also an important link in bipolar disorder,¹² neurodegenerative disorders,¹³ and chronic inflammation.¹⁴ Therefore, small-molecule inhibitors of GSK-3 β may have a therapeutic potential in numerous human diseases. A number of drug discovery programs have yielded small-molecule ATP-competitive inhibitors that are presently in various stages of development.¹⁵

The aim of this study was to find new chemical scaffolds with putative inhibitory potency on GSK-3 β inhibitors. Recent enrichment study in the active site of six GSK-3 β X-ray structures has shown poor results without considering induced fit effect.¹⁶ Actually, the complexity of protein–ligand complex free energy interactions dictates that many significant approximations must be utilized. There are some limitations to use only automated docking-based virtual screening.¹⁷ In this study, we apply ligand-based sequential virtual screening (SQSP),¹⁸ which was started with the HipHop¹⁹ pharmacophore-based virtual screening and was followed by additional screening model. It would be expected to screen a large amount of library in a short time and with more reliable enrichment. Figure 1 shows the strategy; (1) all known

Keywords: GSK-3 β (glycogen synthase kinase-3) inhibitors; HipHop; RP (recursive partitioning); SQSP (sequential virtual screening).

* Corresponding author. Tel.: +82 02 958 5185; fax: +82 02 958 5189; e-mail: anpae@kist.re.kr

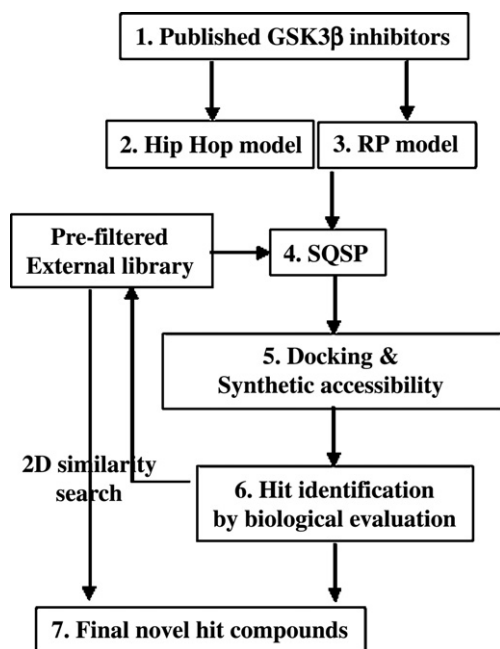


Figure 1. Flowchart of the sequential virtual screening process.

GSK-3 β inhibitor antagonists were collected, (2) Hip-Hop pharmacophore model was generated with carefully selected small sets of known inhibitors, (3) recursive partitioning (RP) model²⁰ was built by comparing the known inhibitors against a set of decoys, (4) virtual screening by the models was conducted sequentially against an external library, (5) some compounds from step 4 were selected considering predicted docking pose and synthetic accessibility, and (6) hit compounds were identified via biological assay process. In summary, the pharmacophore-based initial virtual screening screens a database by checking essential functional features in a molecule, and the RP-based virtual screening discriminated between active and inactive compounds by evaluating molecular topological pattern. The RP model is very attractive in that it utilizes property descriptors with continuous value ranges and transforms these descriptors into a binary classification scheme and gives the resulting decision tree, which makes it easy to split active and inactive compounds by non-statisticians.

2. Results and discussion

2.1. Generation of the best common feature model

For the HipHop pharmacophore analysis, highly active GSK-3 β inhibitors were chosen as per the description in the computational method section. The active ligands with different structure adopt different binding mode to maximize their interaction in active site, and all active ligands do not have same functional groups. Thus, all possible pharmacophore models were inspected by altering the parameter options elucidating if some compounds reflect all features. In HipHop generation, the molecules are going to be used to construct the pharmacophore configuration space that can be specified

Table 1. The common feature hypotheses and corresponding hit rates against active and inactive compounds

Pharmacophores	Pharmacophore composition ^a	Actives (287)	Inactive (994)
A	RHDA	172 (60%)	369 (37%)
B	HDAAA	130 (45%)	175 (18%)
C	RDAAA	120 (42%)	260 (26%)

Their hit rates were evaluated by performing virtual screening against all known 287 GSK-3 β inhibitors and 994 inactive compounds obtained from in-house HTS.

^a A, hydrogen bond acceptor; D, hydrogen bond donor; H, hydrophobic group; R, aromatic ring.

through setting the ‘principal’ compound parameter. This parameter can adopt the values of 0, 1, or 2. A value of 2 means this molecule will be used to build the configuration space. A value of 0 means this molecule will be ignored when building the configuration space. A value of 1 indicates to the program that the molecule can be used to build the configuration space. But whether this molecule is actually used will depend on the setting of other parameters, such as Misses and CompleteMisses. ‘Misses’ means that hypotheses that fail to map completely to more than one training compound will be disallowed. ‘CompleteMisses’ specify the number of molecules that do not have to map to any features in the hypothesis. The Misses and CompleteMisses were varied from 1 to 3, respectively. The value for MaxOmitFeat was set to 2 so that a pharmacophore can be kept even if that specific molecule is a complete miss to that pharmacophore.

Table 1 reports the diverse pharmacophore model compositions collected from the repeated trials and their hit rate against active and inactive compounds. Figures 2 and 3 show the pharmacophore models. The pharmacophore A showed superior hit rate than the other models. However, we selected the pharmacophore B as the best pharmacophore model for virtual screening because the pharmacophore A is non-selective and tends to capture too much false positive hits compared to pharmacophore B. The pharmacophore B appeared to give more effective discrimination against poorly potent inhibitors. The best pharmacophore query was comprised of three hydrogen bond acceptors, one hydrogen bond donor, and one hydrophobic feature as depicted in Figure 3. To check the reliability of pharmacophore model by comparing the binding mode, the inhibitor 4 was aligned onto the best pharmacophore model and was docked into the active site of crystal structure (19ou.pdb) using FlexX program. The hydrogen bond acceptor and donor features on the maleimide ring are generated from hydrogen bond with D133 and V135, respectively. The hydrogen bond acceptor on pyrazine ring was consistent with the fact that such feature interacts with the backbone of D200 burrowing into hydrophobic pocket. The hydrogen bond acceptor on the substitution butyl-alcohol came from the interaction with the NH of Q185. The hydrogen bonding interaction between pyridine ring and R141 was investigated in only docking study but not the pharmacophore model. The hydrophobic feature on flipped pyridine ring was assigned instead of hydrogen

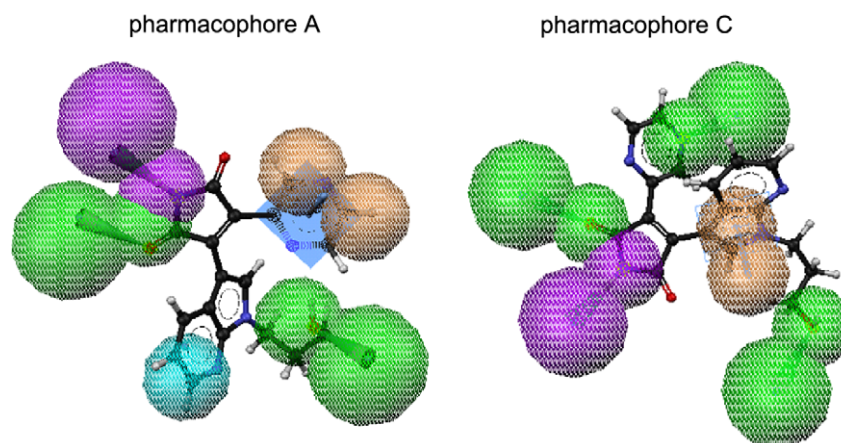


Figure 2. The generated pharmacophore models A and C (cyan: hydrophobic groups; green: hydrogen bond acceptor feature with a vector in the direction of the putative hydrogen donor; orange: aromatic ring; purple: hydrogen bond donor feature with a vector in the direction of the putative hydrogen acceptor).

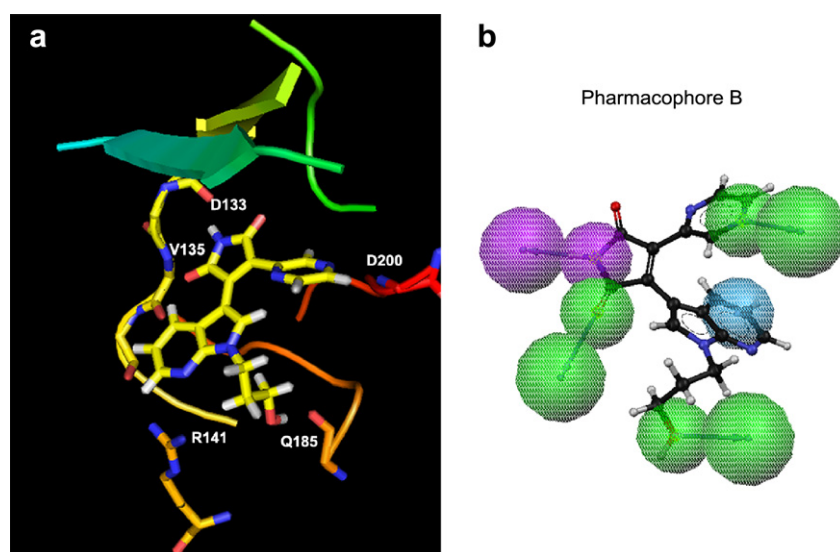


Figure 3. The comparison between the best HipHop model and docking pose. The training compound **4** docked into active site of GSK-3 β crystal structure (a), and mapped onto the pharmacophore model generated (b).

Table 2. Statistical results produced from the final RP model

	# of compounds (%) ^a	Class%Obscorr ^b	Overall%Precorr ^c	Enrichment ^d
Inactive class	4034 (93.25)	95.07	99.58	1.07
Active class	292 (6.75)	94.52	58.11	8.61

^a The number of samples in each class.

^b Intraclass prediction.

^c Overall prediction.

^d The enrichment factor: Overall%Precorr divided by the original percentage of compounds belonging to that class (%).

bond acceptor. It would allow striking more diverse chemical structure since the R141 showed significant movement in various crystal structures.

2.2. Recursive partitioning tree for post-filtering

To classify the hit compounds from the common feature pharmacophore-based virtual screening into active or inactive class, the recursive partitioning model was developed using the two-dimensional descriptors im-

ing molecular shape information. The statistical results for the best RP model are demonstrated in Table 2. The resulting model was determined by variation of parameters described in Section 4, trying to increase following values. The definition, ‘Class%ObsCorr’, is a measure of the number of compounds correctly predicted to belong to a class as a percentage of the total number of compounds observed to be in each class. The measure of ‘Overall%PredCorr’ represents the total number of compounds correctly classified divided by the

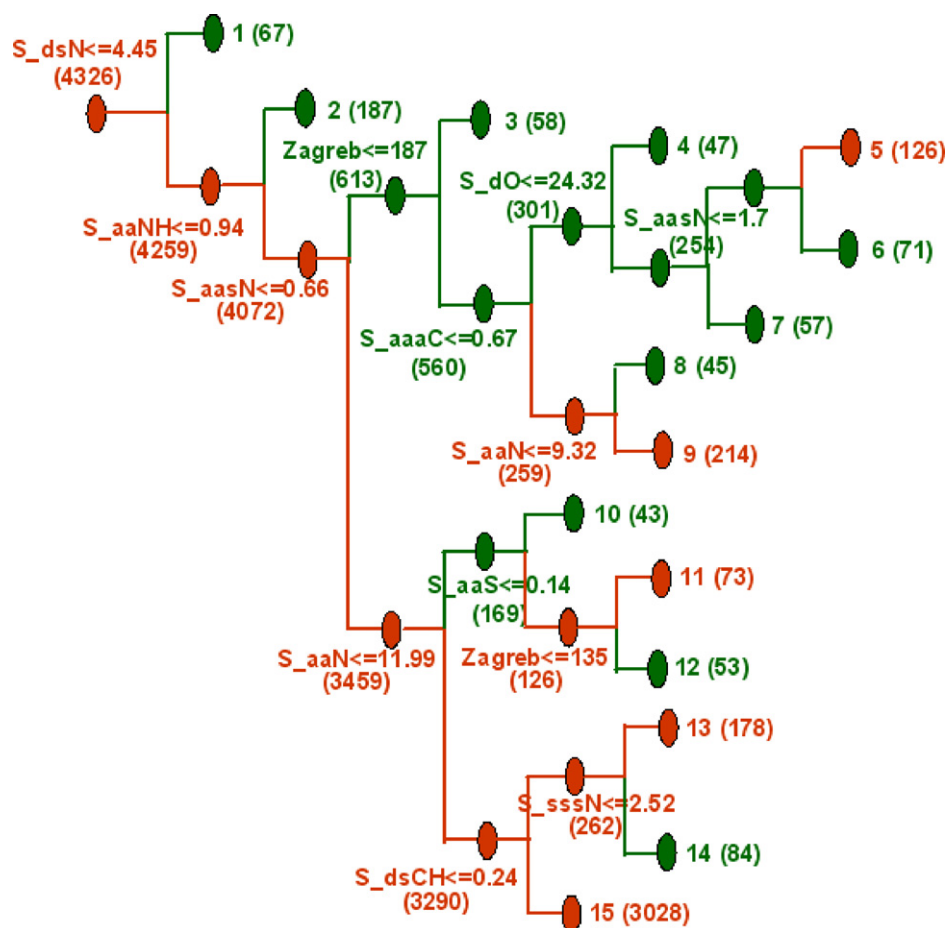


Figure 4. RP tree generated to discriminate active and inactive compounds. At each node (decision point), molecules were split into higher or lower responses according to their descriptors. The red color indicates inactive class, and active class is plotted using green color.

number of compounds predicted to belong to each class. The enrichment factor for a specific class is the ratio of the 'Overall%PredCorr' to the original percentage of compounds belonging to that class.

The statistical indicators suggested that more than eight-fold improvement over random selection could be achieved by application of the resultant RP model. Furthermore, its sequential application after initial virtual screening makes it possible to decrease the number of candidate compounds for experimental assay to a small number in a much more efficient way relative to cherry-picking. Figure 4 displays the optimized RP model by the encouraged descriptors to extract active GSK-3 β inhibitors. All 10 orthogonal descriptors, 9 *E*-state key values and 1 topological index, were required to achieve the observed performance. The first key descriptor is electrotopological value (*E*-state key) computed for each atom in a molecule which encodes information about both the topological environment of that atom and the electronic interactions due to all other atoms in the molecule. That is, the information of the electron accessibility at that atom and the degree of adjacency or topological state of the atom were provided by *E*-state key. The meaning of the *E*-state symbols in the Cerius² implementation is as follows: *S*, sum of numerical value for following atom type; *s*, single bond; *d*, double bond;

t, triple bond; *a*, aromatic bond. Here, the chemical environment around aromatic carbon and nitrogen, and sulfonamide moiety distributed to discriminate be-

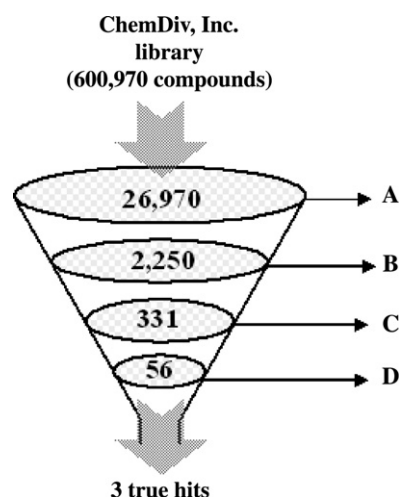


Figure 5. The number of compounds reduced for each sequential screening step. (A) Pre-filtering of raw library by drug-likeness, ADME properties, (B) pharmacophore-based virtual screening, (C) filtration by recursive partitioning tree, (D) final selection considering docking pose and synthetic accessibility.

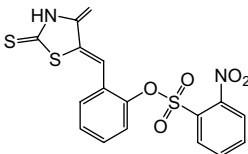
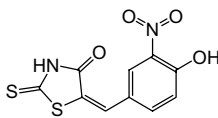
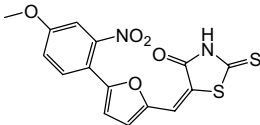
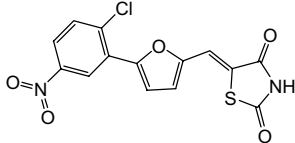
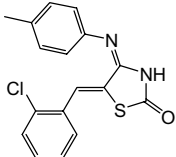
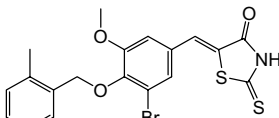
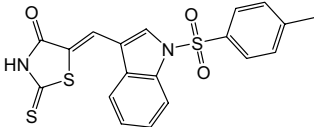
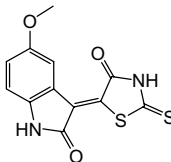
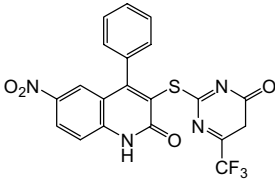
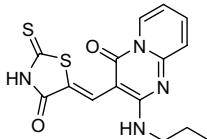
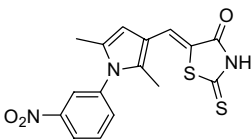
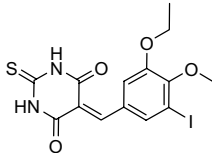
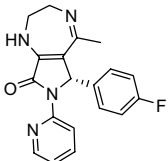
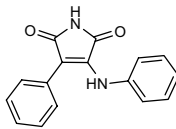
tween active and inactive category. The other main topological descriptor splitting the data set is the Zagreb characterizing the degree of atomic branching in a molecule. These 2D descriptors are beneficial in that 3D shape query directed from the compounds is more restricted.

2.3. Virtual screening using external library

To identify potential new GSK-3 β inhibitors, SQSP was performed using the external library: ChemDiv library (600,970 compounds). The restricting number of a target-focused database would be crucial for efficient handling and realistic analysis of chemical information. Therefore, pre-processing of total library was carried

out to escape time-consuming conformation generation step for pharmacophore-based virtual screening. The filtering standards such as drug-likeness and ADME properties as described in Section 4 are also beneficial for selecting final hit compounds at the end of screening. Figure 5 shows the virtual screening procedure and hit reductions in each step. After filtering one-twentieth of the putative library, by the fast flexible database search tool in Catalyst program and RP classification sequentially, the pharmacophore-based virtual screening stroked 2250 compounds matched onto the best pharmacophore model. Second, the initial hit compounds were put into the RP model as prediction set and 331 of hit compounds were predicted to have an increased probability of being active by eliminating large number of compounds to be

Table 3. Inhibition data of hit compounds from SQSP against ChemDiv library

Compound	Structure	Activity (%) ^a	Compound	Structure	Activity (%) ^a
7		14	8		7
9		5	10		8
11		18	12		6
13		67	14		84
15		41	16		95
17		41	18		58
19		99	Ref.		(IC ₅₀ , 0.52 μ M)

^a Protein kinases were assayed with 10 μ M of test compounds in the presence of 15 μ M of ATP. The remaining enzyme activities were shown by percent activity.

Table 4. IC₅₀ values of selected compounds

Compound	IC ₅₀ (μM)
7	1.56
8	3.97
9	5.56
10	>10
11	>10
12	>10
13	>10

inactive compounds. Third, the final 56 of hit compounds were carefully selected considering docking pose, structural diversity, and synthetic accessibility. Several hit compounds having diverse structure and their binding affinity (percent inhibition at 10 μM of test compounds) for human GSK-3β protein are shown in Table 3. Based on the percent inhibition values, total seven compounds were selected and the activities were evaluated by IC₅₀ value (Table 4). The best hit compound 7 is visualized in its respective pharmacophore model and the most generically stable docking pose in Figure 6. It fulfills the best pharmacophore, by matching perfectly three hydrogen bond acceptors and one donor. The docking pose and conformation of the compound aligns well with the results from ligand-based approach. It also shows the conserved interaction with the important residues, such as D133, V135, and R141, as in the other crystal complexes.

3. Conclusions

A successful virtual screening application was presented revealing novel, micromolar GSK-3β inhibitors. The approach was based on a smart virtual screening strategy, SQSP, which was conducted by combining common feature pharmacophore hypothesis and recursive partitioning model, a classification method as the algorithmic tools. Three-dimensional distances among pharmacophoric features and two-dimensional topological indices mediating molecular shape information were combined as the descriptors. As the results, the ultimate hit compounds have been proposed for biological testing, three

compounds of them showed micromolar inhibitory activity. Their binding mode and interactions of the best hit compound were further analyzed via docking and revealed close similarity to the complexed GSK-3β inhibitor.

4. Materials and methods

4.1. Generation and validation of common feature pharmacophore model

The common feature hypothesis, HipHop pharmacophore model, is the automated tool within Catalyst that is based on alignment of common features present in highly potent compounds. For HipHop pharmacophore analysis for published GSK-3β inhibitors, six compounds were carefully selected as shown in Figure 7 considering the activity, structural rigidity, and diversity.^{21–25} The conformational models of selected compounds having up to 250 conformers were built using the ‘best conformer generation’ method with a 20 kcal/mol energy cutoff.²⁶ HipHop pharmacophore models are derived by comparing a set of conformational models and a number of three-dimensional configurations of chemical features shared among the training set molecules. The parameter setting of Maximum Omitted Features, Misses, and Complete Misses was varied to generate multiple hypotheses in which some compounds may or may not fit all features. Four chemical functions with hydrogen bonding acceptor, aromatic ring, positive ionizable, and hydrophobic group were used as the pharmacophoric feature. The hypothesis generation process in Catalyst was returned 10 possible pharmacophore hypotheses having different arrangement of constituent features or ranking score. After deleting the redundant hypotheses that have the same chemical characteristics and nearly the same distances between these functions, diverse configurations of hypotheses were selected according to ranking scores and fitting scores. The best hypothesis was determined by the potential of discriminating between active and inactive compounds. As an active data set, all known 287 GSK-3β inhibitors were downloaded as SD file format from

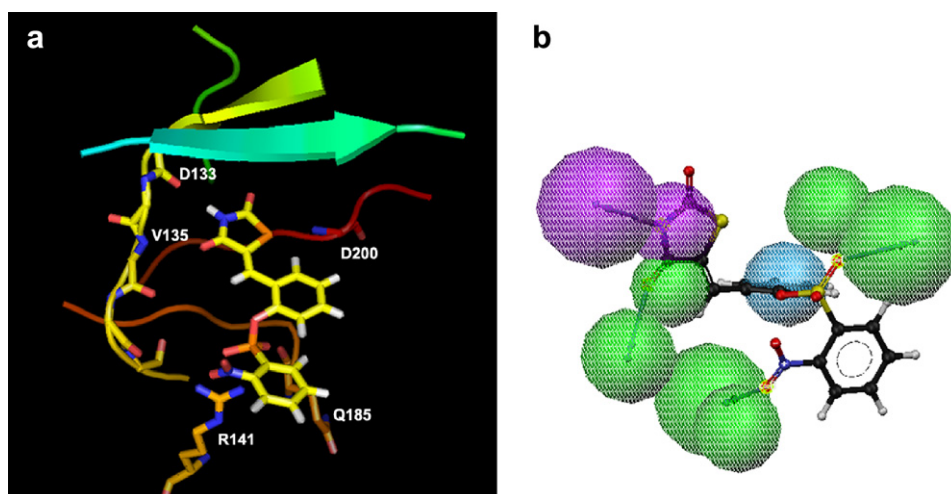


Figure 6. Novel GSK-3β inhibitor mapped the best pharmacophore model and docked into the active site.

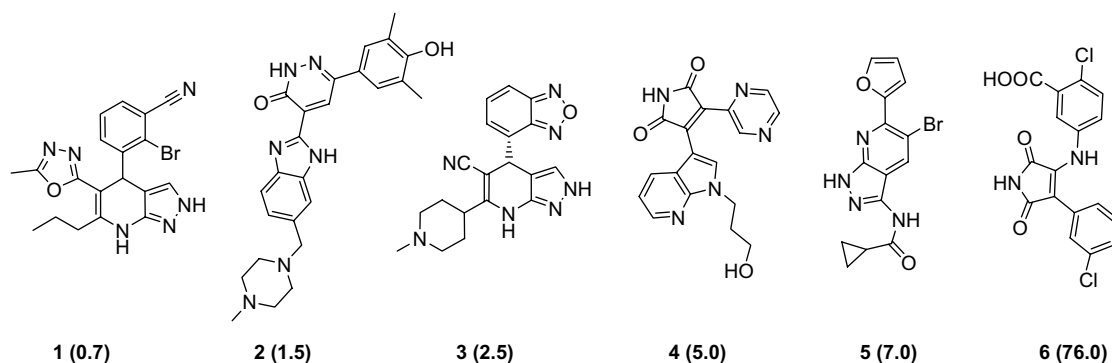


Figure 7. The structures and activities (IC₅₀, nM) of the training GSK-3β inhibitors used for pharmacophore generation.

Integrity database of Prous²⁷ and were converted as the Catalyst database. Total 994 inactive compounds were obtained from in-house HTS experimental results of a kinase-focused library (Asinex).²⁸

4.2. Generation of recursive partitioning model

The RP model was generated using the CART algorithm implemented in Cerius² program.²⁹ The true positive GSK-3β inhibitors were set as active class, and the inactive compounds obtained from HTS were selected as inactive class. To build realistic model covering structural diversity, the GPCR-focused 3040-membered library from Tripos Inc.³⁰ was added as inactive class. The GPCR-focused library may include several active GSK-3β inhibitors, but they might be a negligible quantity. The RP tree was constructed by *E*-state key and topological descriptors based on chemical graph theory. The activity classes were weighted equally, and the splits were scored using Gini Impurity scoring function. The pruning factor values were varied between 3 and 6. The value of 1/1000 of samples was considered as the minimum number of samples in any node. The various values were used for maximum tree depth (layers ≤10) and the default values were accepted for maximum number of generic splits (30), and the number of knots per variable (20). The optimum decision tree was determined by standards described in our previous report.³¹

4.3. Molecular docking

To perform screening and validation of the hits obtained from SQSP, FlexX-based molecular docking study was carried out in the ligand binding sites of 1H8F, 1O9U, 1Q4L, and 1UV5. Receptor description file (RDF) was created within the area of 6.5 Å around the cocrystallized ligand and the core interactions (Val135 and Asp133) were defined in the RDF. For a comparative analysis of the hits obtained in SQSP, FlexX score, G_score [34], PMF_score [35], D_sorce [36], and Chem_score [37] were estimated using the C-score module of the Sybyl7.3.1.³²

4.4. Virtual screening using external library

Virtual screening has been carried out by sequential virtual screening procedure (SQSP) to obtain new com-

pounds with desired activity profiles. The commercial library of ChemDiv Inc.³³ has been utilized for virtual screening. To save screening time and hit selection time, the raw database was preprocessed by drug-likeness (Lipinski's rule of 5), structural diversity, and ADME properties. The drug-likeness and structural diversity were examined using the Hivolt tool in SYBYL program. The in silico ADME properties of each hit compound were calculated by the PreADME program, which was implemented with the back-propagation method on the artificial neural network.³⁴ The tuned database was converted into the Catalyst multiconformational data format in CHARMM-like force field. The best pharmacophore model was used for virtual screening experiment by selecting the fast flexible database search option. Resulting hit lists were put into the second screening model, recursive partitioning tree. The first screening figured out new compounds with similar functional and spatial properties defined in 3D pharmacophore query. The subsequent second screening extracted probably active compounds by comparing topological properties of initial hit lists with those of known compounds. Finally, the final hit compounds were selected by considering synthetic accessibility and predicted binding mode by docking using FlexX program.

4.5. Biological evaluation

The inhibitory activities of the virtual hit compounds were determined against human GSK-3β enzyme. In a final reaction volume of 25 μL, GSK-3β (h) (5–10 mU) is incubated with 8 mM MOPS, pH 7.0, 0.2 mM EDTA, 20 μM YRRAAVPPSPSLSRHSSPHQS(p)EDEEE (phospho GS2 peptide), 10 mM MgAcetate, and [γ-³³P-ATP] (specific activity approx. 500 cpm/pmol, concentration as required). The reaction is initiated by the addition of the MgATP mix. After incubation for 40 min at room temperature, the reaction mixture is stopped by the addition of 5 μL of a 3% phosphoric acid solution. Ten microliters of the reaction is then spotted onto a P30 filtermat and washed three times for 5 min in 50 mM phosphoric acid and once in methanol prior to drying and scintillation counting.

Acknowledgment

This work was supported by Seoul R&BD Program.

References and notes

1. Coghlan, M. P.; Culbert, A. A.; Cross, D. A.; Corcoran, S. L.; Yates, J. W.; Pearce, N. J.; Rausch, O. L.; Murphy, G. J.; Carter, P. S.; Roxbee Cox, L.; Mills, D.; Brown, M. J.; Haigh, D.; Ward, R. W.; Smith, D. G.; Murray, K. J.; Reith, A. D.; Holder, J. C. *Chem. Biol.* **2000**, *7*, 793–803.
2. Woodgett, J. R. *EMBO J.* **1990**, *9*, 2431–2438.
3. Lau, K. F.; Miller, C. C.; Anderton, B. H.; Shaw, P. C. *J. Pept. Res.* **1999**, *54*, 85–91.
4. Embi, N.; Rylatt, D. B.; Cohen, P. *Eur. J. Biochem.* **1980**, *107*, 519–527.
5. Eldar-Finkelman, H.; Schreyer, S. A.; Shinohara, M. M.; LeBoeuf, R. C.; Krebs, E. G. *Diabetes* **1999**, *48*, 1662–1666.
6. Eldar-Finkelman, H. *Trends Mol. Med.* **2002**, *8*, 126–132.
7. Hanger, D. P.; Hughes, K.; Woodgett, J. R.; Brion, J. P.; Anderton, B. H. *Neurosci. Lett.* **1992**, *147*, 58–62.
8. Takashima, A.; Yamaguchi, H.; Noguchi, K.; Michel, G.; Ishiguro, K.; Sato, K.; Hoshino, T.; Hoshi, M.; Imahori, K. *Neurosci. Lett.* **1995**, *198*, 83–86.
9. Liao, X.; Zhang, L.; Thrasher, J. B.; Du, J.; Li, B. *Mol. Cancer Ther.* **2003**, *2*, 1215–1222.
10. Ghosh, J. C.; Altieri, D. C. *Clin. Cancer Res.* **2005**, *11*, 4580–4588.
11. Ougolkov, A. V.; Fernandez-Zapico, M. E.; Savoy, D. N.; Urrutia, R. A.; Billadeau, D. D. *Cancer Res.* **2005**, *65*, 2076–2081.
12. Zarate, C. A., Jr.; Singh, J.; Manji, H. K. *Biol. Psychiatry* **2006**, *59*, 1006–1020.
13. Martinez, A.; Castro, A.; Dorronsoro, I.; Alonso, M. *Med. Res. Rev.* **2002**, *22*, 373–384.
14. Hoefflich, K. P.; Luo, J.; Rubie, E. A.; Tsao, M. S.; Jin, O.; Woodgett, J. R. *Nature* **2000**, *406*, 86–90.
15. Meijer, L.; Flajolet, M.; Greengard, P. *Trends Pharmacol. Sci.* **2004**, *25*, 471–480.
16. Gadakar, P. K.; Phukan, S.; Dattatreya, P.; Balaji, V. N. *J. Chem. Inf. Model.* **2007**. doi:10.1021/ci6005036.
17. Schneider, G.; Bohm, H. J. *Drug Discov. Today* **2002**, *7*, 64–70.
18. Engels, M. F.; Thielemans, T.; Verbinen, D.; Tollenaere, J. P.; Verbeeck, R. *J. Chem. Inf. Comput. Sci.* **2000**, *40*, 241–245.
19. CATALYST 4.11 User Guide, Accelrys, San Diego, CA, USA, 2006.
20. Breiman, L.; Friedman, J. H.; Olshen, R. A.; Stone, C. J. *Classification and Regression Trees*; Wadsworth International Group: Belmont, CA, 1984.
21. Kohara, T.; Fukunaga, K.; Hanano, T. MITSUBISHI, Preparation of dihydropyrazolopyridines as glycogen synthase kinase-3b (GSK-3b) inhibitors, WO 2004014910.
22. Schoenafinger, K.; Hoelder, S.; Will, D.W.; Matter, H.; Mueller, G.; Bossart, M. AVENTIS, Production of 4-benzimidazol-2-yl-pyridazin-3-one derivatives and use thereof in medicaments, WO 2005085230.
23. O'Neill, D. J.; Shen, L.; Prouty, C.; Conway, B. R.; Westover, L.; Xu, J. Z.; Zhang, H. C.; Maryanoff, B. E.; Murray, W. V.; Demarest, K. T.; Kuo, G. H. *Bioorg. Med. Chem.* **2004**, *12*, 3167–3185.
24. Witherington, J.; Bordas, V.; Haigh, D.; Hickey, D. M.; Ife, R. J.; Rawlings, A. D.; Slingsby, B. P.; Smith, D. G.; Ward, R. W. *Bioorg. Med. Chem. Lett.* **2003**, *13*, 1581–1584.
25. Bertrand, J. A.; Thieffine, S.; Vulpetti, A.; Cristiani, C.; Valsasina, B.; Knapp, S.; Kalisz, H. M.; Flocco, M. *J. Mol. Biol.* **2003**, *333*, 393–407.
26. Smellie, A.; Kahn, S. D.; Teig, S. L. *J. Chem. Inf. Comput. Sci.* **1995**, *35*, 285–294.
27. Prous Integrity Database, copyright 1995–2004 Prous Science; <http://www.prous.com>.
28. <http://www.asinex.com>.
29. Cerius² 2.41, User Guide, Accelrys, San Diego, CA, USA, 2006.
30. LeadQuest Chemical Compound Libraries; Tipos: St. Louis, MO, 2000.
31. Kim, H. J.; Choo, H.; Cho, Y. S.; Koh, H. Y.; No, K. T.; Pae, A. N. *Bioorg. Med. Chem.* **2006**, *14*, 2763–2770.
32. Tripos Inc. *HiVol, SYBYL 7.3*; St. Louis, MO 63144.
33. <http://www.chemdiv.com>.
34. PreADME, ver 1.1.2; B138A, Yonsei Engineering Research Complex, Yonsei University 134 Sinchon-dong, Seodaemun-gu, Seoul 120-749, Korea.